ELSEVIER

Journal of Power Sources 66 (1997) 101–105

JOURNAL OF POWER SOURCES

Characteristics of nickel–metal hydride cells containing metal hydride alloys prepared by an atomization technique

H.S. Lim [a,*], G.R. Zelter [a], D.U. Allison [a], R.E. Haun [b]

[a] *Hughes Space and Communications Company, Torrance, CA 90509, USA*

[b] *Retech, A Division of LESAT, Ukiah, CA, USA*

Received 20 March 1996; revised 30 August 1996

Abstract

We have studied effects of inert gas atomization and optional annealing of hydride-forming alloys on the alloy performance as the anode material of an Ni/MH_x cell. Metal hydride electrodes were prepared using atomized powder of several hydride-forming alloys and studied for their performances in a flooded electrolyte Ni/MH_x cell. Their performance was compared, at various temperatures, with that of corresponding non-atomized alloys. The performance studied included: specific capacity as a function of discharge rates; rate capability; cycle performance; particle size, and physical degradation with cycling. The atomized alloys showed lower specific capacity and slower activation with cycling than corresponding non-atomized alloys. A post-atomization annealing treatment improved both in specific capacity and activation process, but the improvement was not sufficient enough to match the performance of the non-atomized alloys. Rate capability of $La_{0.7}Ce_{0.3}Ni_{3.2}Co_{1.0}Mn_{0.6}Al_{0.2}$ alloy was not affected significantly by the atomization. Rate capability at 20 °C of another alloy with only a slight variation in composition, $La_{0.7}Ce_{0.3}Ni_{3.3}Co_{1.0}Mn_{0.4}Al_{0.3}$, was reduced a little by the atomization, while that at 2 °C was not affected. A direct observation of the physical degradation process of alloy particles was possible using the atomized powder particles due to their well-defined spherical geometry.

Keywords: Metal hydride alloys; Nickel; Atomization techniques

1. Introduction

A nickel–metal hydride (Ni/MH_x) cell is a storage battery cell which is rapidly emerging in recent years for many applications, especially for consumer electronics. An Ni/MH_x cell is an alkaline storage cell and is similar in many aspects to a nickel–cadmium (Ni/Cd) cell, which has been the main workhorse for many electronic devices. The Ni/MH_x system has recently received a special attention from many battery developers and manufacturers especially due to environmental safety concerns regarding the Ni/Cd cell, while general demands for a reliable portable power source are ever increasing. Concerns about toxicity of cadmium have led to stricter government environmental regulations both in production processes and disposal of the cells. Such regulations made it more difficult to manufacture Ni/Cd cells and dispose of them economically after use. For most applications a storage cell is generally preferred to a primary cell due to the disposal problem. The Ni/MH_x cell has higher gravimetric and volumetric energy densities than Ni/Cd cells by approximately 30%. The Ni/MH_x cell has also the advantage of being able to replace an Ni/Cd cell virtually without a change of the existing power systems for many electronic devices because they are similar in physical structure as well as in the charge and discharge voltage characteristics.

Ni/MH_x cells are now available from several battery manufacturers. However, further improvements of the cell are desired for long cycle life, low self-discharge, and operation at an elevated temperature. Performance of the cell for these characteristics is closely related to the alloy properties. Therefore, it is highly desirable to improve the hydride alloy material for an improved Ni/MH_x cell. Preparation technique of the alloys as well as their composition has been reported to affect the performance [1,2]. Most popular preparation techniques of the alloy powder are arc-melting and melting in an induction furnace followed by a mechanical pulverization of the resulting ingots. It has been reported that an AB_5-type alloy prepared by a rapid cooling technique resulting in small grain (approximately 10 μm) columnar structure give longer cycle life than an equiaxed, large grain (approximately 50 μm) structure from a slow cooling technique [3]. Atomization of a molten alloy [4,5] will be a logically preferred

* Corresponding author.

PII S0378-7753(96)02488-3

technique to prepare a rapid-cooled alloy. As an effort to develop an advanced Ni/MH_x cell [6,7], the present report describes results of a new preparation technique of alloy material for the anodes of a nickel–metal hydride cell.

2. Experimental

2.1. Alloy compositions

The hydride alloy compositions studied in this report included: $La_{0.8}Ce_{0.2}Ni_{4.75}Sn_{0.25}$, $La_{0.8}Ce_{0.2}Ni_{3.75}Co_{1.0}Sn_{0.25}$, and $La_{1-x}Ce_xNi_yCo_zMn_uAl_v$ where $x=0.2$–0.5, $y=3.2$–3.55, $z=0.75$–1.0, $u=0.4$–0.6, and $v=0.2$–0.3. The alloy powder preparation techniques were either arc-melting followed by a mechanical pulverization or atomization of the melt. 'Non-atomized powder' was prepared by mechanical pulverization of alloy ingots in a stainless-steel mortar followed by sieving in a nitrogen filled glove box. Elemental analyses of the alloys were carried out by d.c. plasma analysis technique. Results of the metal analyses of the alloy powder agreed well with the intended composition within an experimental error (a few % for the major components and within 10% for the minor components). However, the oxygen content was much higher (2000–3000 ppm) in some atomized alloys ($La_{0.8}Ce_{0.2}Ni_{4.75}Sn_{0.25}$) which were prepared by initial preliminary runs than in the non-atomized alloys (100–200 ppm). Later results with an alternate equipment with improved vacuum control showed considerably reduced oxygen content (220–270 ppm) but it was still a little higher than that of a non-atomized powder.

2.2. Atomization

The basic scheme of the atomization technique is shown in Fig. 1. Atomization was carried out in a water-cooled copper crucible by passing molten alloy through an orifice in an inert atmosphere (helium or argon) while an inert gas jet is directed at the molten stream of the alloy. The orifice size was 0.94 to 1.25 cm in diameter. The inert gas nozzle was approximately 0.2 cm in inner diameter. The inert atmosphere chamber at near atmospheric pressure typically contained

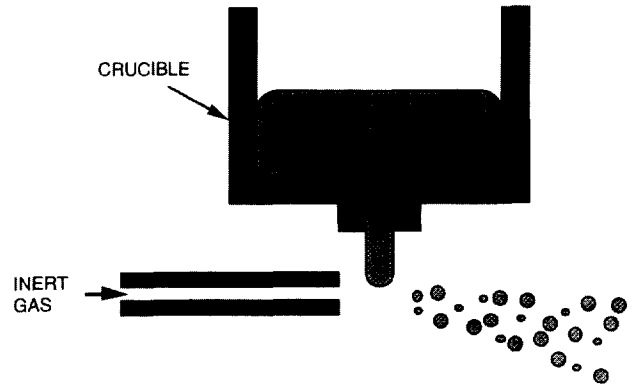

Fig. 1. A schematic drawing of atomization technique.

Fig. 2. SEM picture of typical atomized powder (The scale bar in the picture is for 10 μm.)

4–10 ppm of oxygen and approximately 30 ppm of H_2O. The helium gas for the atomization runs contained typically 2.5 ppm of oxygen and approximately 8 ppm of H_2O. The source gas pressure varied from 100 to 400 psi. Resulting alloy powders with various particle size were collected and sieved through sieves of various sizes. Typical test samples were in the particle size range of 38–90 μm (−170+400 mesh) unless otherwise specified. A scanning electron microscope (SEM) picture of typical atomized powder is shown in Fig. 2. The atomized alloys were also annealed in a rhenium boat in an inert atmosphere for 72 h at 1100 °C in order to improve their specific capacity. The annealed powder was found to be sintered together to form a cake. The sintered cake was mechanically broken and sieved to prepare powder of desired particle size.

2.3. Test electrodes and cells

The metal hydride (MH_x) electrodes for evaluation of the alloys were prepared by pasting a slurry of the alloy powder, Shawinigan acetylene black (AB50), and polymer solution on a piece of nickel foam substrate of 80 to 100 pores per inch. Test electrodes were approximately 2.3 cm × 2.3 cm in size. Each electrode contained approximately 0.8 to 1 g of alloy. Performance tests of the MH_x electrodes are carried out in a flooded electrolyte Ni/MH_x cell containing 31 wt.% KOH electrolyte. After activation, the cells were immediately trickle charged at 10 to 20 mA for a minimum of several hours before measuring their initial capacities to prevent possible corrosive oxidation of the active alloy material.

2.4. Test cycle regime

Capacity tests were carried out by charging test cells at 165 mA for 2.5 h followed by discharge of the cells at the same rate to 1.0 V. The standard cycling test regime was an aerospace low earth orbit (LEO) regime at approximately 50% depth-of-discharge with 110% recharge, i.e., 35 min discharge at 0.86*C* rate (285 mA) followed by recharge at 0.60*C* (198 mA) for 55 min.

3. Results

We have studied effects of atomization and an optional annealing, as a preparation technique, on the performance of hydride-forming alloys as the anode material of an Ni/MH_x cell. Measured values of the specific electrochemical capacity of the present hydride-forming alloys depended rather strongly on their preparation techniques. The rate of activation process also depended strongly on the preparation techniques. It takes many cycles to reach full capacity values, especially for those prepared by the atomization. Some alloys take several hundreds of cycles before they are fully activated. In this activation period, measured values of the electrode capacity, especially from one electrode to another, were not reproducible. It is difficult to make precise comparison of capacities of different alloys due to the lack of reproducibility of the measurements and especially due to the fact that the number of cycles needed to reach the maximum capacity is different for individual alloys. The effect of alloy preparation techniques on the specific capacity is shown in Table 1 by comparing approximate values of the maximum specific capacities of alloys. The specific capacities of the atomized powder were much lower than those of corresponding non-atomized alloys. The specific capacity of the atomized powder was improved the annealing, but only marginally as shown in Table 1.

3.1. Effects of discharge rates and temperature on performance

Effects of discharge rate and temperature on cell performance for both atomized and non-atomized alloys were studied at various rates ranging from approximately 0.2 to 1*C* rate at temperatures of 2, 10, and 20 °C. As the discharge rate increases, the average cell voltage and the capacity are depressed, while the degree of the inter-dependence varied with the individual alloys. Measured specific capacity values of atomized and non-atomized alloys at various temperatures are shown as a function of discharge rates in Figs. 3–6. Discharge capacity decreased roughly linearly with increase of discharge rate with the exception of the non-atomized $La_{0.7}Ce_{0.3}Ni_{3.3}Co_{1.0}Mn_{0.4}Al_{0.3}$ alloy at 20 °C (see Fig. 5). Even though the specific capacities are reduced by the atom-

Table 1
A comparison of maximum capacities of various alloy

Sample identifiction	Maximum measured capacity (mAh/g)	Comments
$La_{0.8}Ce_{0.2}Ni_{4.75}Sn_{0.25}$	240	Non-atomized
$La_{0.8}Ce_{0.2}Ni_{4.75}Sn_{0.25}$	176	Atomized
$La_{0.7}Ce_{0.3}Ni_{3.2}Co_{1.0}Mn_{0.6}Al_{0.2}$	329	Non-atomized
$La_{0.7}Ce_{0.3}Ni_{3.2}Co_{1.0}Mn_{0.6}Al_{0.2}$	190	Atomized
$La_{0.7}Ce_{0.3}Ni_{3.2}Co_{1.0}Mn_{0.6}Al_{0.2}$	268	Atomized, annealed
$La_{0.7}Ce_{0.3}Ni_{3.3}Co_{1.0}Mn_{0.4}Al_{0.3}$	321	Non-atomized
$La_{0.7}Ce_{0.3}Ni_{3.3}Co_{1.0}Mn_{0.4}Al_{0.3}$	200	Atomized
$La_{0.7}Ce_{0.3}Ni_{3.3}Co_{1.0}Mn_{0.4}Al_{0.3}$	231	Atomized, annealed

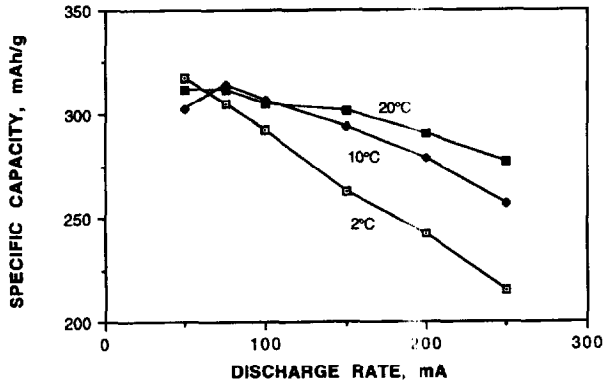

Fig. 3. Specific capacity of non-atomized $La_{0.7}Ce_{0.3}Ni_{3.2}Co_{1.0}Mn_{0.6}Al_{0.2}$ alloy at 2, 10, and 20 °C at various discharge rates.

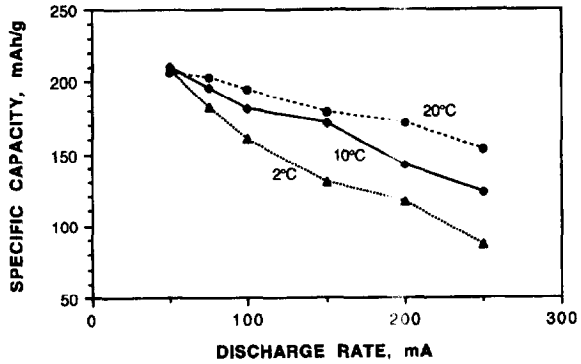

Fig. 4. Specific capacity of atomized $La_{0.7}Ce_{0.3}Ni_{3.2}Co_{1.0}Mn_{0.6}Al_{0.2}$ alloy at 2, 10, and 20 °C at various discharge rates.

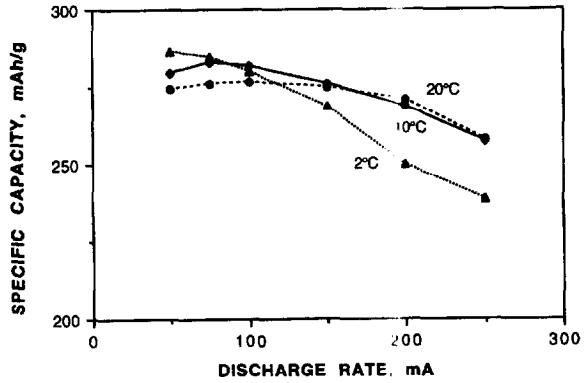

Fig. 5. Specific capacity of non-atomized $La_{0.7}Ce_{0.3}Ni_{3.3}Co_{1.0}Mn_{0.4}Al_{0.3}$ alloy at 2, 10, and 20°C at various discharge rates.

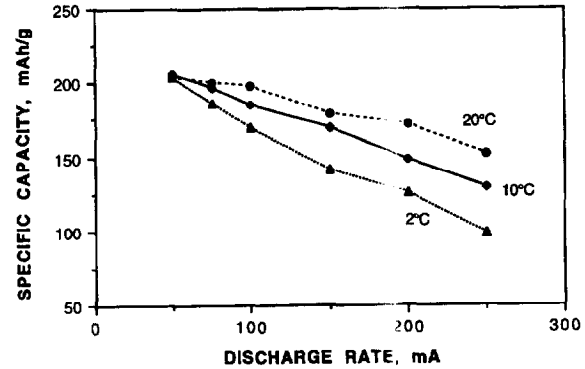

Fig. 6. Specific capacity of atomized $La_{0.7}Ce_{0.3}Ni_{3.3}Co_{1.0}Mn_{0.4}Al_{0.3}$ alloy at 2, 10, and 20 °C at various discharge rates.

ization, the relative rate capability of the atomized alloy, $La_{0.7}Ce_{0.3}Ni_{3.2}Co_{1.0}Mn_{0.6}Al_{0.2}$, remains approximately the same as that of the corresponding non-atomized alloy (cf. Fig. 3 versus Fig. 4), while that for the alloy, $La_{0.7}Ce_{0.3}Ni_{3.3}Co_{1.0}Mn_{0.4}Al_{0.3}$, was slightly deteriorated by the atomization (cf. Fig. 5 versus Fig. 6).

Effects of charge temperature on cell voltage and capacity were studied by charging cells at various temperatures followed by discharging at 20 °C. Charging temperatures between 0 and 20 °C had little effect on either cell voltage or capacity but charging at 30 °C or higher showed reduced capacity. Effects of discharge temperature on cell voltage and capacity were studied by charging cell at 20 °C followed by discharging at various temperatures. Discharge temperatures between 10 and 40 °C did not show a significant effect on capacity or voltage. However, both capacity and voltage were depressed noticeably when the cell was discharged at 0 °C.

3.2. Effects of particle size on performance

Particle size range for this study was rather limited because particle sizes bigger than approximately 100 μm (150 mesh) were not suitable for electrode fabrication. We have tested electrodes containing alloy powders in three different size ranges, i.e., below 38, 38–63, and 63–90 μm. The size below 38 μm did not give full capacity. Electrodes containing large particles (63–90 μm) showed higher capacity and faster activation than those containing small particles (38–63 μm).

3.3. Effects of atomization and annealing on cycle life performance

We have studied the effects of atomization and alternate annealing on the cycle life performance of the alloys. Typical cycle life performances of non-atomized and atomized alloys are shown in Fig. 7. Electrodes with non-atomized powders activate faster and have a much higher initial capacity than the corresponding atomized alloys. An X-ray diffraction study on the atomized alloys indicated that the alloy is amorphous. After annealing the alloy at 1100 °C for 72 h it became partially crystalline [8]. It is speculated that the lack of crystalinity is mainly responsible for the low capacity of the atomized alloys. However, a long-term cycling (hundreds of cycles) showed that capacities of the non-atomized alloys are decreasing with cycling, while the atomized alloys showed a trend of increase in capacity. Annealing improved the rate of activation process considerably for alloys, $La_{0.7}Ce_{0.3}Ni_{3.2}Co_{1.0}Mn_{0.6}Al_{0.2}$ and $La_{0.7}Ce_{0.3}Ni_{3.3}Co_{1.0}Mn_{0.4}Al_{0.3}$, but still required over 100 cycles for full activation.

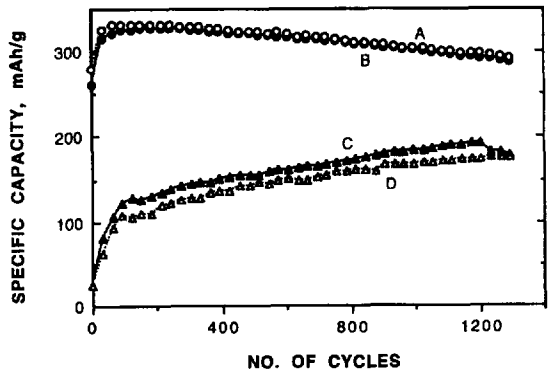

Fig. 7. Effects of atomization on cycle life performance of MH_x electrodes. Alloy: $La_{0.7}Ce_{0.3}Ni_{3.2}Co_{1.0}Mn_{0.6}Al_{0.2}$. (A), (B) non-atomized powder of 63–90 μm, and (C), (D) atomized powder of 38–63 μm in diameter.

3.4. Physical degradation of alloy particles with cycling

Physical degradation process of the atomized alloy particles with the electrochemical cycling in an Ni/MH_x cell was studied by taking SEM pictures of alloy particles from a cycled electrode which were separated by dissolving the polymer bonding agent of the electrode. The SEM pictures of the particles after various number of cycles are shown in Figs. 8 and 9. The mechanical degradation of $La_{0.8}Ce_{0.2}Ni_{3.55}Co_{0.75}Mn_{0.4}Al_{0.3}$ alloy particles after 387 cycles was minimal as shown in Fig. 8. After 862 cycles, the mechanical

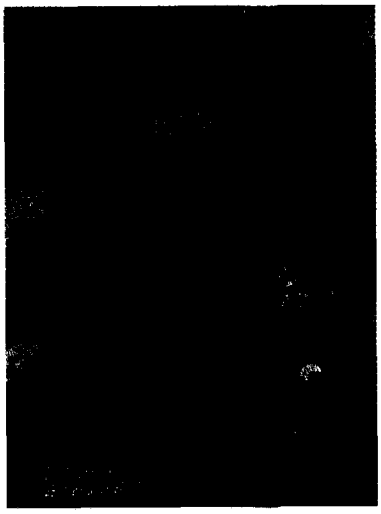

Fig. 8. SEM picture of $La_{0.8}Ce_{0.2}Ni_{3.55}Co_{0.75}Mn_{0.4}Al_{0.3}$ alloy in particle size 63–90 μm in diameter after 387 cycles. (The scale bar in the picture is for 10 μm.)

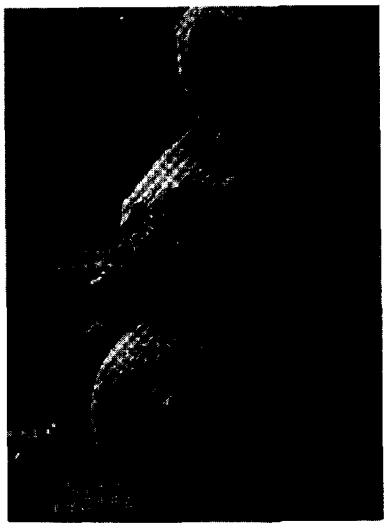

Fig. 9. SEM picture of $La_{0.5}Ce_{0.5}Ni_{3.55}Co_{0.75}Mn_{0.4}Al_{0.3}$ alloy in particle size 63–90 μm in diameter after 862 cycles. (The scale bar in the picture is for 10 μm.)

disintegration process of the particles through surface cracking is readily visible for $La_{0.5}Ce_{0.5}Ni_{3.55}Co_{0.75}Mn_{0.4}Al_{0.3}$ alloy as shown in Fig. 9.

4. Summary

We have studied specific capacity as a function of discharge rates, rate capability, cycle performance, particle size, and physical degradation with cycling. The atomized alloys showed lower specific capacity and slower activation with cycling compared with corresponding non-atomized alloys. A post-atomization annealing treatment improved both in specific capacity (Table 1) and activation process, but the improvement was not sufficient enough to reach the performance of the non-atomized alloys. Rate capability of $La_{0.7}Ce_{0.3}Ni_{3.2}Co_{1.0}Mn_{0.6}Al_{0.2}$ alloy was not affected significantly by the atomization. Rate capability at 20 °C of an alternate alloy having slightly different composition, $La_{0.7}Ce_{0.3}Ni_{3.3}Co_{1.0}Mn_{0.4}Al_{0.3}$, was reduced a little by the atomization, while that at 2 °C was not affected. A direct observation of the physical degradation process of alloy particles was possible using the atomized powder particles due to their well-defined spherical geometry.

Present results do not appear to be sufficient to draw a conclusion about the possible merits of the atomization technique, even though overall performances of the non-atomized alloys were superior to those of the atomized alloy. Further studies are needed, especially for reducing the oxygen contents in the atomized alloys and for cycle life performance of the alloys prepared by an improved atomization technique.

Acknowledgements

This work is supported by US Department of Energy Grant No. DE-FG03-93ER1430.

References

[1] G.G. Libowitz, An introduction to metallic hydrides and their applications, in D. Corrigan and S. Srinivasan (eds.), *Proc. Symp. Hydrogen Storage Materials, Batteries, and Electrochemistry*, Proc. Vol. 92-5, The Electrochemical Society, Pennington, NJ, USA, p. 3.

[2] T. Sakai, H. Yoshinaga, H. Miyamura, N. Kuriyama and H. Ishikawa, *J. Alloys Comp., 180* (1992) 37–54.

[3] T. Sakai, T. Hazama, H. Miyamura, N. Kuriyama, A. Kato and H. Ishikawa, *J. Less-Common Met., 172–174* (1991) 1175–1184.

[4] T. Murada and K. Koshiro, Hydrogen absorbing electrode characteristics of Ti–Ni alloy powder prepared by gas atomization process, *GS New Tech. Rep., 50* (1) (1991) 21–29.

[5] H. Hasebe, *Eur. Patent No. 420 669* (4 Apr 1991).

[6] H.S. Lim, D.F. Pickett, J.F. Stockel, and J.J. Smithrick, Advanced nickel–metal hydride cell development at Hughes — A joint work with US government, *Conf. NASA Centers for Commercialization and Development of Space, Albuquerque, NM, USA, 8–12 Jan. 1995; Proc. 10th Annual Battery Conf. Applications and Advances, 10–13 Jan. 1995, Long Beach, CA, USA*, p. 65.

[7] H.S. Lim, Status of advanced nickel–metal hydride cell development, *Space Battery Workshop, Albuquerque, NM, USA, 17–19 Apr. 1995.*

[8] J.J. Reilly, unpublished result.